HHS Public Access

Author manuscript

Anal Chem. Author manuscript; available in PMC 2015 June 27.

Published in final edited form as:

Anal Chem. 2015 May 19; 87(10): 5095–5100. doi:10.1021/ac504151e.

Nanopipet-Based Liquid–Liquid Interface Probes for the Electrochemical Detection of Acetylcholine, Tryptamine, and Serotonin via Ionic Transfer

Michelle L. Colombo, **Jonathan V. Sweedler**, and **Mei Shen**[*]

Department of Chemistry, University of Illinois at Urbana–Champaign, 600 South Matthews Avenue, Urbana, Illinois 61801, United States

Abstract

A nanoscale interface between two immiscible electrolyte solutions (ITIES) provides a unique analytical platform for the detection of ionic species of biological interest such as neurotransmitters and neuromodulators, especially those that are otherwise difficult to detect directly on a carbon electrode without electrode modification. We report the detection of acetylcholine, serotonin, and tryptamine on nanopipet electrode probes with sizes ranging from a radius of ≈7 to 35 nm. The transfer of these analytes across a 1,2-dichloroethane/water interface was studied by cyclic voltammetry and amperometry. Well-defined sigmoidal voltammograms were observed on the nanopipet electrodes within the potential window of artificial seawater for acetylcholine and tryptamine. The half wave transfer potential, $E_{1/2}$, of acetylcholine, tryptamine, and serotonin were found to be −0.11, −0.25, and −0.47 V vs $E_{1/2,TEA}$ (term is defined later in experimental), respectively. The detection was linear in the range of 0.25–6 mM for acetylcholine and of 0.5–10 mM for tryptamine in artificial seawater. Transfer of serotonin was linear in the range of 0.15–8 mM in LiCl solution. The limit of detection for serotonin in LiCl on a radius ≈21 nm nanopipet electrode was 77 μM, for acetylcholine on a radius ≈7 nm nanopipet electrode was 205 μM, and for tryptamine on a radius ≈19 nm nanopipet electrode was 86 μM. Nanopipet-supported ITIES probes have great potential to be used in nanometer spatial resolution measurements for the detection of neurotransmitters.

[*]**Corresponding Author:** Phone: +1 (217) 300-3587. mshen233@illinois.edu.

Supporting Information

Parameters for pulling nanometer orifice pipets; cyclic voltammogram of 1 mM acetylcholine and SEM image of pipet to show diffusion coefficient determination; cyclic voltammogram of 1 mM tryptamine and SEM image of pipet to show diffusion coefficient determination; cyclic voltammogram of 1 mM serotonin and SEM image of pipet to show diffusion coefficient determination; cyclic voltammogram of serotonin in artificial seawater; Cyclic voltammograms of dopamine, ascorbic acid, γ-aminobutyric acid in artificial seawater and LiCl, with cyclic voltammogram of TEA shown as reference; calibration curve for cyclic voltammetry of acetylcholine; calibration curve for cyclic voltammetry of tryptamine; calibration curve for amperometry of acetylcholine; calibration curve for amperometry of tryptamine; calibration curve for cyclic voltammetry of serotonin; calibration curve for amperometry of serotonin. This material is available free of charge via the Internet at http://pubs.acs.org.

Author Contributions

All authors have given approval to the final version of the manuscript

Notes

The authors declare no competing financial interest.

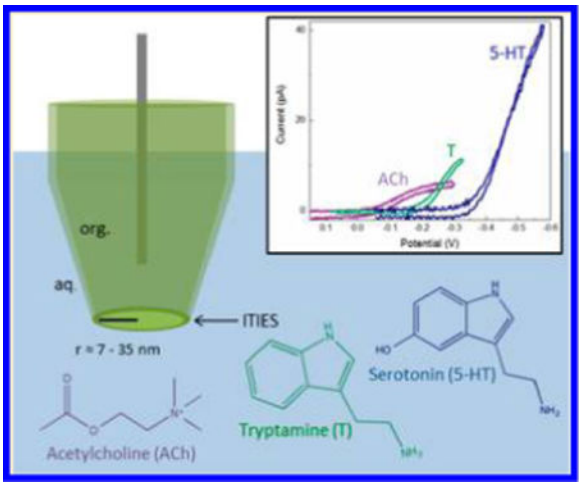

Neurotransmitters, acting as chemical messengers, play an important role in neurotransmission, which governs many functional aspects of nervous system activity, including behaviors, emotional responses, learning, and memory. Specifically, acetylcholine (ACh) is a key regulator in sleep and wakefulness,[1,2] as well as consciousness,[3] and promotes sustained attention.[4] Similarly, disruptions in the serotonergic system have been shown to be involved in disorders such as anxiety and depression,[5–7] and the neuromodulator tryptamine (T) has been shown to enhance serotonin (5-HT) release.[8]

Electrochemical measurements of neurotransmitters[9–23] have been successful in providing insights concerning neuronal function and processes such as exocytosis. Current electrochemical detection of neurotransmitters is based on Faradaic electron transfer on a carbon electrode; thus, mainly redox-active neurotransmitters are detected, e.g., dopamine and serotonin. Electrochemical detection of nonredox active neurotransmitters (e.g., ACh) is achieved indirectly using an electrode modified with enzyme, where a combination of acetylcholine esterase and choline oxidase is needed and the kinetics of the enzyme reaction can limit the electrode response.[24–27] Methods for direct detection of nonredox active neurotransmitters (e.g., without electrode modification) need to be developed.

The use of pipet electrodes based on ionic transfer across an interface between two immiscible electrolyte solutions (ITIES)[28–41] has been an important method to detect ionic analytes. Ionic transfer of neurotransmitters across ITIES, mainly micro- and macrointerfaces has been reported.[42–44] NanoITIES-based sensor probes have significantly improved spatial resolution compared to microelectrodes and have been proven to be useful for imaging a single nanopore.[45] A typical nanoITIES sensor probe consists of a laser-pulled pipet with a pore radius in the nanometer scale that can be filled with an organic solution and immersed into biologically relevant fluids. Upon polarization, charged neurotransmitters of interest can be transferred from one phase to another, which is the basis for ionic species sensing. Because these sensors rely on ion transfer, as opposed to faradaic electron transfer, nonelectroactive transmitters can be identified and quantitatively measured.

To the best of our knowledge, the ionic transfer of neurotransmitters across a nanointerface has not been reported. Herein we describe the direct quantitative and qualitative detection of both electrochemically nonredox-active (ACh) and redox-active neurotransmitters (T and 5-HT) with nanoITIES- based pipet sensor probes. Such an approach has the advantage of being able to detect both electrochemically nonredox-active neurotransmitters (e.g., ACh) and redox-active neurotransmitters (e.g., T and 5-HT) (Scheme 1).

EXPERIMENTAL SECTION

Reagents

Potassium tetrakis(pentafluorophenyl)borate (TFAB) was obtained from Boulder Scientific Company (Mead, CO). Tetradodecylammonium (TDDA) chloride, tetraethylammonium chloride (TEACl), 1,2-dichloroethane (1,2-DCE), and chlorotrimethylsilane were purchased from Sigma-Aldrich (St. Louis, MO). The TFAB salt of TDDA (TDDATFAB) was prepared by metathesis. Potassium chloride (KCl) was from VWR (Radnor, PA), calcium chloride ($CaCl_2$) was from Sigma-Aldrich (St. Louis, MO), and magnesium chloride ($MgCl_2$) was from Amresco (Solon, OH). Magnesium sulfate ($MgSO_4$), HEPES, and lithium chloride (LiCl) were from Fisher Scientific (Pittsburgh, PA). Artificial seawater (ASW) contained (in mM) the following: 460 NaCl, 10 KCl, 10 $CaCl_2$, 22 $MgCl_2$, 26 $MgSO_4$, and 10 HEPES (pH 7.8). Acetylcholine (ACh) chloride and tryptamine (T) hydrochloride were from Sigma-Aldrich (St. Louis, MO), and serotonin (5-HT) hydrochloride was purchased from Alfa Aesar (Ward Hill, MA). All reagents were used as received, and solutions were prepared using 18.3 MΩ cm deionized water (ELGA, Woodridge, IL). The prepared solutions were passed through a 0.2 μm filter (Thermo Scientific, Waltham, MA) before use.

Nanopipet Electrode Preparation and Characterization

Nanometer-scale pipet probes were fabricated by laser pulling of quartz capillaries (O.D. = 1.0 mm, I.D. = 0.7 mm, length = 10 cm, Sutter Instrument, Novato, CA) using a P-2000 capillary puller (Sutter Instrument) using the parameters listed in Table S1 in Supporting Information. To make sure a stable interface was formed at the orifice of the nanopipet, we applied a surface treatment through a chemical vapor silanization process via chlorotrimethylsilane to the pulled nanopipet. For the surface treatment, the pulled nanopipets were placed on a Petri-dish that was put into a plastic desiccator, where a vacuum was created, and chlorotrimethylsilane was introduced immediately after the vacuum with a three-way valve. Nanopipets were backfilled using a Hamilton syringe, and the interface was pushed to the tip of the pipet by creating a gentle vibration using an alligator clip. Pipets were characterized using scanning electron microscopy (SEM) and ion-transfer voltammetry. For SEM imaging, the nanopipets were coated with a thin Au/Pd film by a high-resolution sputter coater (Quorum Technologies LTD, Kent, UK), and the orifices were observed by high resolution field emission SEM (FEI dual-beam 235, FEI Co., Hillsboro OR) under a 20 kV electron beam. Figure 1A shows one nanopipet probe with a radius ≈15 nm, and Figure 1B shows an SEM image of the orifice of the pipet tip. The prepared nanopipets were filled with a 1,2-DCE solution of organic supporting electrolytes and immersed in an aqueous solution of either ACh, T, or 5-HT.

Electrochemical Experiments

The transfer of protonated ACh, T, and 5-HT across the 1,2-DCE/water interface was studied by cyclic voltammetry and amperometry. All electrochemical measurements were recorded using a CHI1205B Electrochemical Analyzer (CH Instruments, Austin, TX). A nanopipet was filled with 5 mM TDDATFAB in 1,2-DCE and immersed into an aqueous solution for the detection of neurotransmitters (NT). NTs were detected in an aqueous solution of ASW. ASW was used, as it is a relevant biological media for our commonly used neuronal model, *Aplysia californica*;[46,47] by optimizing our detection in this media, future biological experiments will be facilitated. When NT cannot be transferred within the potential window of ASW, an aqueous media with a potential window larger than that of ASW was used, i.e., LiCl. A Pt wire (diameter = 50 μm) was inserted inside the pipet, and either a Ag wire (diameter =250 μm) coated with AgCl or a Au wire (diameter =50μm) coated with polypyrrole (Ppy) was placed outside the pipet used as an external reference electrode; the voltage was applied between the platinum wire and the external reference electrode. The Pt wire was electrochemically etched until the end was small enough to be placed approximately 200 μm away from the pipet tip. cell 1, cell 2, and cell 3 represent the electrochemical cells for different aqueous background solutions and reference electrodes used in this study. At the end of each experiment, TEACl was added as an internal standard to determine the transfer potentials of each analyte.

$$\text{cell 1:Pt}|5\text{ mM}\quad \text{TDDATFAB}+1,2-\text{DCE}\|\text{ASW}+x\text{mM NT}|\text{Ppy}|\text{Au}$$

$$\text{cell 2:Pt}|5\text{ mM}\quad \text{TDDATFAB}+1,2-\text{DCE}\|10\text{ mM LiCl}+x\text{ mM NT}|\text{AgCl}|\text{Ag}$$

$$\text{cell 3:Pt}|5\text{ mM}\quad \text{TDDATFAB}+1,2-\text{DCE}\|\text{ASW}+x\text{ mM NT}|\text{AgCl}|\text{Ag}$$

The diffusion coefficients of ACh, T (in ASW), and 5-HT (in LiCl) were calculated using pipets with radii on the scale of hundreds of nanometers, which were easily verified via SEM. Several pipets of this size were used to measure the steady-state current response for each analyte at 1 mM concentration (Figures S1, S2, and S3 in Supporting Information show the cyclic voltammogram for one of the pipets used, e.g., radius = 360, 450, and 340 nm for ACh, T, and 5-HT, respectively). Diffusion coefficients could then be calculated using the expression[48]

$$i=4xnFDca \quad (1)$$

where i is the steady-state limiting current, x is a function of the quantity $RG = r_g/a$ (r_g and a are outer and inner tip radii, respectively)[49], n is the number of transferred charges in the tip reaction, F is Faraday's constant, a is the radius of the pipet, D is the diffusion coefficient of the neurotransmitter measured, and c is the concentration of analyte in solution. A proposed disk geometry for the nanopipet tip was used for the calculation. The diffusion coefficients of ACh and T in ASW were found to be $7.5 \pm 1.2 \times 10^{-6}$ cm^2/s and $6.1 \pm 0.4 \times 10^{-6}$ cm^2/s

at 24 °C, respectively, in ASW. The diffusion coefficient for 5-HT in 10 mM LiCl was found to be $6.3 \pm 0.8 \times 10^{-6}$ cm^2/s at 24 °C. The same relationship was then used in determining the radius of each of the smaller scale pipets used for the detection of neurotransmitters.

Limits of detection (LODs) were calculated by $3s/m$,[50] where s is equal to the standard deviation of background solution without neurotransmitters present and m is equal to the slope of the calibration curve. In the case of cyclic voltammetry, s was determined by the standard deviation of the average current at a potential on the limiting current from three replicate cyclic voltammograms of background solution. In the case of amperometry, s was determined by the standard deviation of the average current obtained over a 50 s amperometric i–t curve of background solution.

RESULTS AND DISCUSSION

Cyclic voltammetry was used to determine the half-wave transfer potentials ($E_{1/2}$) of acetylcholine (ACh), tryptamine (T), and serotonin (5-HT). Upon applying a potential, the neurotransmitters were transferred voltammetrically across the nanopipet-supported ITIES tip, and their cyclic voltammograms are shown in Figure 2; the transfer of all three neurotransmitters investigated produced sigmoidal voltammograms, with $E_{1/2}$ as −0.11, −0.25, and −0.47 vs $E_{1/2,TEA}$ for ACh, T, and 5-HT, respectively. As shown in Figure 2, the transfer of ACh and T (Figure 2a) occurred well before the background, while 5-HT is much more difficult to be transferrred, and its transfer has slight overlap with background. For this reason, background subtraction is used to increase the accuracy of measurements.

Because ACh transfers early within the potential window of ASW, it can achieve a steady-state current for up to 200 mV before background interference from ASW occurs. Some capacitance is seen in the cyclic voltammogram of ACh, due the small pipet radius of 7 nm and the fact that it was scanned at a rate of 50 mV/s rather than 20 mV/s (Figure 2a). T has a moderate $E_{1/2}$ and was also able to achieve a steady state in ASW (Figure 2b). It is worth noting that the observed difference in the transfer potentials between T and 5-HT corresponds well with that reported in the literature at a much larger nitrobenzene/water interface.[44] Because 5-HT requires a much larger overpotential for its transfer, ASW background interference proves to be an issue for the detection of low concentrations of 5-HT. A 2 mM addition of 5-HT has only a small response relative to ASW, because the two transfer at similar potentials (Figure S4, Supporting Information). Steady-state transfer of lower concentrations of 5-HT was achieved when a background solution of 10 mM LiCl was used in place of ASW, due to the larger potential window of LiCl (Figure 2c).

The different transfer potentials of these protonated analytes on the nano-ITIES probes provide the basis for their qualitative detection. Additionally, the ITIES probes presented here are selective toward the detection of ACh, T, and 5-HT compared to other neurotransmitters that could coexist in vivo, such as dopamine, γ-aminobutyric acid (GABA), and ascorbic acid, a redox-active compound present at high levels in many neuronal systems. The response of these nanopipet probes to these possible interferents are shown in Figures S5 and S6, Supporting Information. The tests were performed both in

ASW and LiCl, background solutions used in this study. It can be seen from Figures S5 and S6 that no change occurred in the shape of the cyclic voltammograms of ASW and LiCl within the relevant potential window when 5 mM DA, 5 mM GABA, or 100 mM AA were added. TEA was added at the end of these interferent tests to verify that each nanopipet electrode was working properly, ensuring that the lack of interferent signal was due to the fact that it does not transfer. Overall, at the ITIES of nanopipet electrode presented here, ascorbic acid, dopamine, and GABA cannot be transferred within the potential window and thus are not detected. In contrast, surface modifications on the traditionally used carbon electrode are often needed to enhance NTs detection selectivity against ascorbic acid, e.g., carbon electrodes modified with Nafion were used for 5-HT detection in the presence of ascorbic acid.[51–54]

Figure 3 shows the quantitative detection of ACh (Figure 3a and 3b) and T (Figure 3c and 3d) on nanopipet-supported ITIES probes. As shown in Figure 3a, even with such a small interface radius of ≈7 nm, we were able to use cyclic voltammetry to detect ACh quantitatively in the range of 0.25–6 mM, resulting in a steady-state current that was linearly proportional to concentration (Figure S7, $R^2 = 0.994$, Supporting Information). T also showed linear detection using cyclic voltammetry (Figure 3c), in the range of 0.5–10 mM at $a \approx 19$ nm radius interface, with a steady-state current linearly proportional to the concentration (Figure S8, $R^2 = 0.989$, Supporting Information).

Amperometry was also used for the quantification of ACh and T, as shown in Figures 3b and 3d, respectively. Using this technique, probes were held at a potential at which a steady-state current occurred for ACh and T. The resulting average current over a period of 50 s was linearly proportional to ACh concentration from 0.25 to 6 mM (Figure S9, $R^2 = 0.995$, Supporting Information) and linearly proportional to T concentration from 0.5 to 10 mM (Figure S10, $R^2 = 0.992$, Supporting Information). The LODs for ACh and T were calculated to be 205 μM and 86 μM, respectively, based on *i–t* curves.

The quantitative detection of 5-HT in LiCl with both cyclic voltammetry and amperometry are shown in Figure 4a and 4b, respectively. The response is linear over the concentration range of 0.15–8 mM for 5-HT. On the basis of results shown in Figure 4a, limiting current corresponding to detection of 5-HT at −0.51 V is changing linearly with its concentration in the range of 0.15–8 mM (Figure S11, $R^2 = 0.995$, Supporting Information). Similarly, linear calibration curve (Figure S12, $R^2 = 0.999$, Supporting Information) for this concentration range was obtained using amperometry on a radius of ≈21 nm nanopipet electrode by holding the probe at −0.52 V vs $E_{1/2,TEA}$ (Figure 4b), with an LOD of 77 μM. In order for 5-HT to be detected in the potential window of biological media, e.g., ASW, an ionophore can be used to facilitate the transfer of 5-HT; thus, the transfer potential of 5-HT can be shifted to be within the potential window of biological media, namely with the mechanism of facilitated ion transfer. Work is currently in progress to facilitate earlier transfer of 5-HT so that it can be detected in biological media.

CONCLUSIONS

Acetylcholine (ACh), tryptamine (T), and serotonin (5-HT) have been successfully detected quantitatively and qualitatively at a nanopipet-supported interface between 1,2-DCE and aqueous solutions via ionic transfer. Transfer potentials at $E_{1/2}$ were compared between ACh, T, and 5-HT, with the following transfer potential order: ACh < *T* < 5-HT, with ACh being transferred at the least negative potential. A lower detection limit for the detection of 5-HT was observed using a 1,2-DCE/LiCl interface compared to a 1,2-DCE/ASW interface, because transfer of serotonin occurs at a similar potential as ASW background. The local concentrations of ACh and 5-HT from an exocytotic event are well above the LODs of these probes.[55,56] Nanoelectrodes coupled with scanning electrochemical microscopy[57] have successfully provided nanometer spatial resolution imaging of single nanopore[45] and single nanoparticles.[58] The nanopipet electrodes presented here have great potential to be used in detecting neurotransmitters for nanometer scale biological structures, such as synapses and in single vesicles. Overall, as shown in our work, nanopipet-supported ITIES probes can be used as multifunctional sensors to detect both electrochemically nonredox-active and redox-active neurotransmitters in both a qualitative and quantitative manner. The nano-ITIES electrodes presented here are selective toward the detection of ACh, T, and 5-HT against other neurotransmitters that could coexist in vivo, such as dopamine, γ-aminobutyric acid (GABA), and ascorbic acid. Work is currently in progress to use these nano-ITIES probes to image the neurotransmission process using scanning electrochemical microscopy.

Supplementary Material

Refer to Web version on PubMed Central for supplementary material.

Acknowledgments

Research reported in this publication was supported by the National Institute of Neurological Disorders and Stroke of the National Institutes of Health under award number R21NS085665. The content is solely the responsibility of the authors and does not necessarily represent the official views of the National Institutes of Health. J.V.S. is grateful for the support from the National Institutes of Health under award number P30 DA018310. SEM was carried out in the Frederick Seitz Materials Research Laboratory Central Research Facilities, University of Illinois. We thank Prof. Joaquin Rodriguez Lopez for helpful discussions.

REFERENCES

1. Riedel G, Platt B. Behav Brain Res. 2011; 221:499–504. [PubMed: 21238497]
2. Jones BE. Trends Pharmacal Sci. 2005; 26:578–586.
3. Perry R, Perry E, Walker M. Trends Neurosci. 1999; 22:273–280. [PubMed: 10354606]
4. Bruno JP, Himmelheber AM, Sarter M. Cogn Brain Res. 2000; 9:313–325.
5. Lesch KP, Bengel D, Heils A, Sabol SZ, Greenherg BD, Petri S, Benjamin J, Muller CR, Hamer DH, Murphy DL. Science. 1996; 274:1527–1531. [PubMed: 8929413]
6. Pezawas L, Meyer-Lindenberg A, Drabant EM, Verchinski BA, Munoz KE, Kolachana BS, Egan MF, Mattay VS, Hairi AR, Weinbegerger DR. Nat Neurosci. 2005; 8:828–824. [PubMed: 15880108]
7. Caspi A, Sugden K, Moffitt TE, Taylor A, Craig IW, Harrington H, McClay J, Mill J, Martin J, Braithwaite A, Poulton R. Science. 2003; 301:386–389. [PubMed: 12869766]
8. Shimazu S, Miklya I. Prog Neuro-Psychopharmacol Biol Psychiatry. 2004; 28:421–427.
9. Wightman RM, Haynes CL. Nat Neurosci. 2004; 7:321–322. [PubMed: 15048116]

10. Amatore C, Arbault S, Bonifas I, Lemaitre F, Verchier Y. Chem Phys Chem. 2007; 8:578–585. [PubMed: 17243189]
11. Amatore C, Arbault S, Bouret Y, Guille M, Lemaitre F, Verchier Y. ChemBioChem. 2006; 7:1998–2003. [PubMed: 17086558]
12. Anderson BB, Chen G, Gutman DA, Ewing AGJ. Neurosci Methods. 1999; 88:153–161.
13. Chen G, Gavin PF, Luo G, Ewing AGJ. Neurosci. 1995; 15:7747–7755.
14. Chow RH, von Ruden L, Neher E. Nature. 1992; 356:60–63. [PubMed: 1538782]
15. Michael, AC.; Borland, LM., editors. Electrochemical methods for neuroscience. CRC Press; Boca Raton: 2007.
16. Leszczyszyn DJ, Jankowski JA, Viveros OH, Diliberto EJ Jr, Near JA, Wightman RM. L Biol Chem. 1990; 265:14736–14737.
17. Alvarez de Toledo G, Fernandez-Chacon R, Fernandez JM. Nature. 1993; 363:554–558. [PubMed: 8505984]
18. Uchiyama Y, Maxson MM, Sawada T, Nakano A, Ewing AG. Brain Res. 2007; 1151:46–54. [PubMed: 17408597]
19. Haynes CL, Buhler LA, Wightman RM. Biophys Chem. 2006; 123:20–24. [PubMed: 16678962]
20. Wightman RM, Schroeder TJ, Finnegan JM, Ciolkowski EL, Pihel K. Biophys J. 1995; 68:383–390. [PubMed: 7711264]
21. Venton BJ, Wightman RM. Anal Chem. 2003; 75:414A–421A.
22. Adams RA. Anal Chem. 1976; 48:1126–1138.
23. Bruns D, Jahn R. Nature. 1995; 377:62–65. [PubMed: 7659162]
24. Hale PD, Wightman RM. Mol Cryst Liq Cryst. 1988; 160:269–279.
25. Kawagoe JL, Nieaus DE, Wightman RM. Anal Chem. 1991; 63:2961–2965. [PubMed: 1789455]
26. Tamiya E, Sugiura Y, Navera EN, Mizoshita S, Nakajima K, Akiyama A, Karube I. Anal Chim Acta. 1991; 251:129–134.
27. Barkhimer TV, Kirchhoff JR, Hudson RA, Messer WS Jr, Tillekeratne LMV. Anal Bioanal Chem. 2008; 392:651–662. [PubMed: 18773199]
28. Amemiya S, Kim J, Izadyar A, Kabagambe B, Shen M, Ishimatsu R. Electrochim Acta. 2013; 110:836–845.
29. Amemiya, S. Heterogeneous Electron Transfer Reactions. In: Bard, AJ.; Mirkin, MV., editors. Scanning Electrochemical Microscopy. 2. Taylor and Francis; New York: 2012. p. 127-156.Chapter 6
30. Samec Z, Samcová E, Girault HH. Talanta. 2004; 63:21–32. [PubMed: 18969401]
31. Samec Z. Pure Appl Chem. 2004; 76:2147–2180.
32. Senda M, Kakiuchi T, Osakais T. Electrochim Acta. 1991; 36:253–262.
33. Wang Y, Velmurugan J, Mirkin MV, Rodgers PJ, Kim J, Amemiya S. Anal Chem. 2010; 82:77–83. [PubMed: 20000449]
34. Reymond F, Fermín D, Lee HJ, Girault HH. Electrochim Acta. 2000; 45:2647–2662.
35. Rodgers PJ, Amemiya S. Anal Chem. 2007; 79:9276–9285. [PubMed: 18004818]
36. Amemiya S, Bard AJ. Anal Chem. 2000; 72:4940–4948. [PubMed: 11055713]
37. Vanysek P. Anal Chem. 1990; 62:827–835.
38. Mirkin MV, Liu B. Electroanalyis. 2000; 12:1433–1446.
39. Mirkin MV, Liu B. Anal Chem. 2001; 73:670A–677A.
40. Stockmann T, Montgomery JA-M, Ding ZJ. Electroanal Chem. 2012; 684:6–12.
41. Stockmann TJ, Zhang J, Montgomery A-M, Ding Z. Anal Chim Acta. 2014; 821:41–47. [PubMed: 24703212]
42. Arrigan DWM, Ghita M, Benia V. Chem Commun. 2004; 6:732–733.
43. Herzog G, McMahon B, Lefoix M, Mullins ND, Collins CJ, Moynihan HA, Arrigan DWM. J Electroanal Chem. 2008; 622:109–114.
44. Tatsumia H, Ueda T. L Electroanal Chem. 2011; 655:180–183.
45. Shen M, Ishimatsu R, Kim J, Amemiya S. Am Chem Soc. 2012; 134:9856–9859.

46. Fan Y, Lee CY, Rubakhin SS, Sweedler JV. Analyst. 2013; 138:6337–6346. [PubMed: 24040641]
47. Jing J, Sweedler JV, Cropper EC, Alexeeva V, Park JH, Romanova EV, Xie F, Dembrow NC, Ludwar BC, Weiss KR, Vilim FS. J Neurosci. 2010; 30:16545–16558. [PubMed: 21147994]
48. Lefrou C. J Electroanal Chem. 2006; 592:103–112.
49. Kim J, Shen M, Nioradze N, Amemiya S. Anal Chem. 2012; 84:3489–3492. [PubMed: 22462610]
50. Harris, DC., editor. Quantitative Chemical Analysis. 8. W. H. Freeman and Company; New York: 2010.
51. Gerhardt GA, Oke AF, Nagy G, Moghaddam B, Adams RN. Brain Res. 1984; 290:390–395. [PubMed: 6692152]
52. Brazell MP, Kasser RJ, Renner KJ, Feng J, Moghaddam B, Adams RN. J Neurosci Methods. 1987; 22:167–172. [PubMed: 2893860]
53. Hashemi P, Dankoski EC, Petrovic J, Keithley RB, Wightman RM. Anal Chem. 2009; 81:9462–9471. [PubMed: 19827792]
54. Jackson BP, Dietz SM, Wightman RM. Anal Chem. 1995; 67:1115–1120. [PubMed: 7717525]
55. Aidoo AY, Ward K. Math Comput Modell. 2006; 44:952–962.
56. Bunin MA, Wightman RM. L Neurosci. 1998; 18:4854–4860.
57. Bard, AJ.; Mrkin, MV., editors. Scanning Electrochemical Microscopy. Marcel Dekker; New York: 2001.
58. Sun T, Yu Y, Zacher BJ, Mrkin MV. Angew Chem, Int Ed. 2014; 53:1–6.

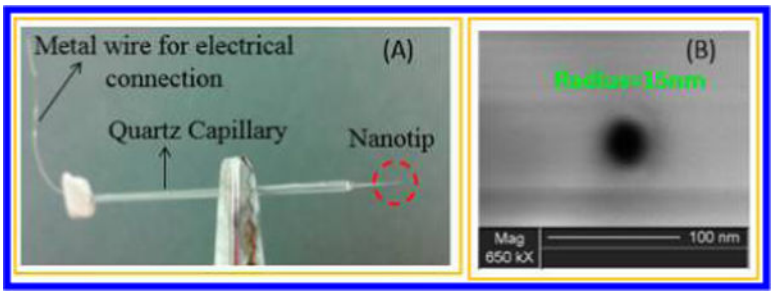

Figure 1.

Photograph (A) and SEM image (B) of a nanopipet prepared in the lab. The pipet was prepared by laser pulling a quartz capillary.

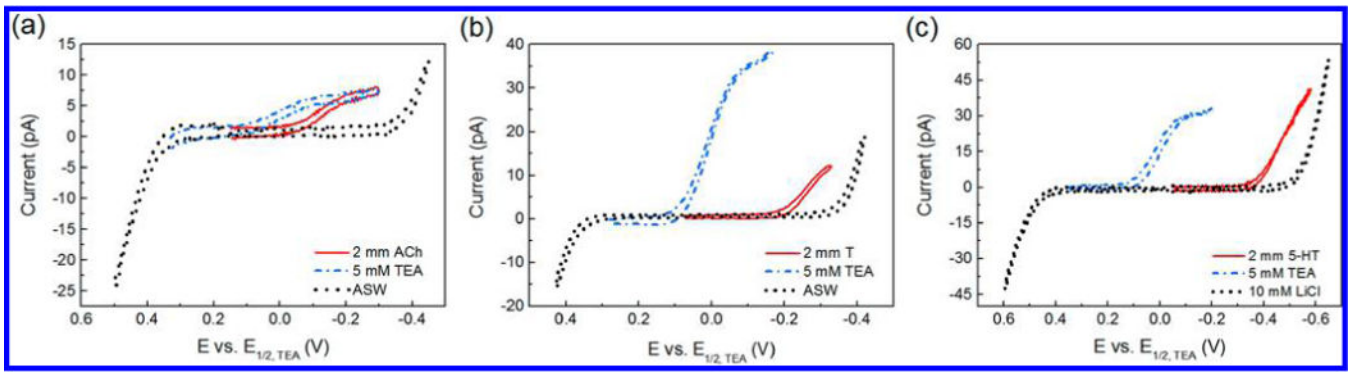

Figure 2.

Cyclic voltammograms of acetylcholine (ACh), tryptamine (T), and serotonin (5-HT) on a nanopipet electrode. (a) 2 mM acetylcholine transfer across a radius ≈7 nm interface in cell 1; scan rate = 0.05 V/s. (b) 2 mM tryptamine transfer across a radius ≈19 nm interface in cell 1; scan rate = 0.02 V/s. (c) 2 mM serotonin transfer across a radius ≈35 nm interface in cell 2; scan rate = 0.05 V/s. For comparison, the cyclic voltammogram of tetraethylammonium is shown in each overlay.

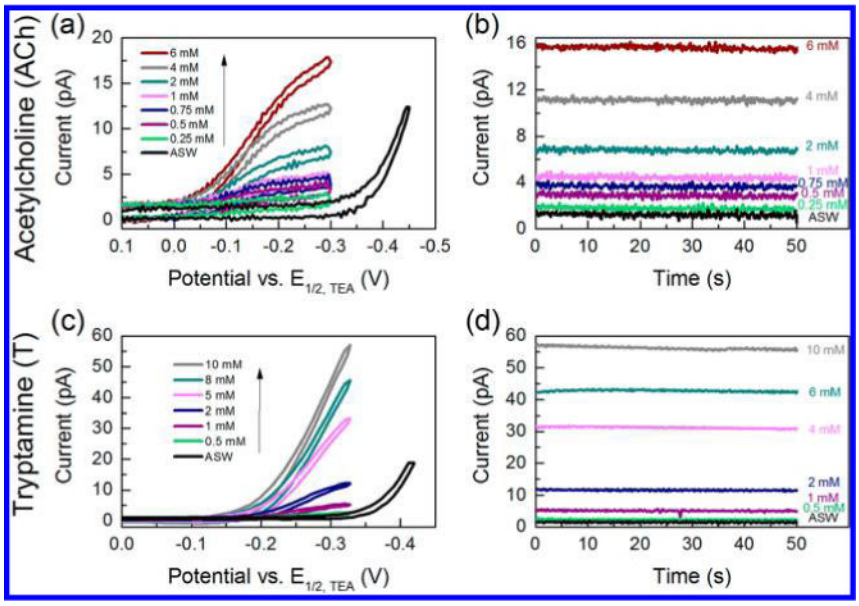

Figure 3.

(a) Cyclic voltammograms and (b) amperometric *i–t* curves for 0.25–6 mM acetylcholine (ACh) using a nanopipet probe with a radius of 7 nm in cell 1; applied potential $E = -0.25$ V vs $E_{1/2,TEA}$ for *i–t* curves. (c) Cyclic voltammograms and (d) amperometric *i–t* curves for 0.5–10 mM tryptamine (T) using a nanopipet probe with a radius of 19 nm in cell 1; applied potential $E = -0.32$ V vs $E_{1/2,TEA}$ for *i–t* curves.

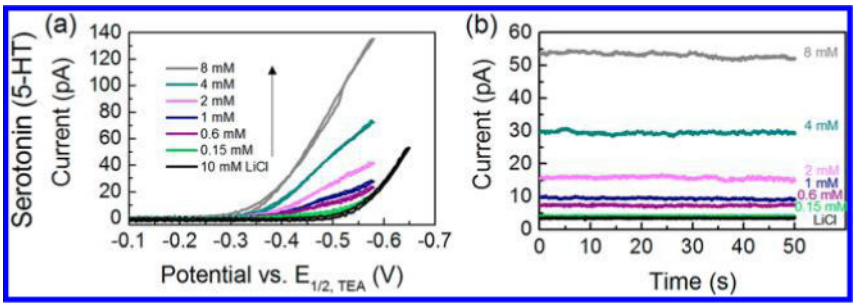

Figure 4.

(a) Cyclic voltammograms of 0.15–8 mM serotonin (5-HT) on a nanopipet electrode with a radius of 35 nm in cell 2. (b) Amperometric *i*–*t* curves for 0.15–8 mM 5-HT using a nanopipet probe with a radius of 21 nm in cell 2; applied potential $E = -0.52$ V vs $E_{1/2,TEA}$.

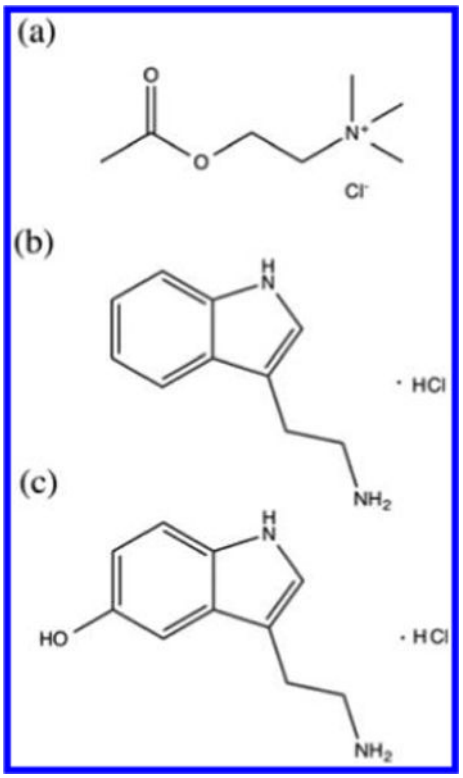

Scheme 1.

Molecular Structure of Protonated (a) Acetylcholine (ACh), (b) Tryptamine (T), and (c) Serotonin (5-HT)